

Negative Differential Resistance, Instability, and Critical Transition in Lightning Leader

Xueqiang Gou^{1†}, Chao Xin¹, Liwen Xu¹, Ping Yuan¹, Yijun Zhang², Mingli Chen³

¹ College of Physics and Electronic Engineering, Northwest Normal University, Lanzhou 730070, China

² Department of Atmospheric and Oceanic Sciences & Institute of Atmospheric Sciences, Fudan University, Shanghai, 200438, China

³ Department of Building Environment and Energy Engineering, The Hong Kong Polytechnic University Hong Kong, SAR, China

[†]Corresponding to: Xueqiang Gou (1491168405@qq.com)

Abstract. The phenomena of leader extinction and restrike during lightning events, such as multiple strokes in ground flashes or recoil leaders in cloud flashes, present significant challenges. A key aspect of this issue involves the discussion of the channel's negative differential resistance and its instability. From the perspective of bifurcation theory in nonlinear dynamics, this paper suggests an inherent consistency among the channel's negative differential resistance, channel instability, and the critical transition from insulation to conduction. This study examines the differential resistance characteristics of the leader-streamer system in lightning development. We correlate the differential resistance characteristics of the leader-streamer channel with the channel's state and instability transitions, investigating the critical current and potential difference conditions required for the stable transition of the leader-streamer channel.

Key words: negative differential resistance; instability; critical transition; lightning

1 Introduction

Natural lightning exhibits distinct intermittent characteristics that differentiate it from long-gap discharges observed in laboratory settings (Gou et al., 2010; Gou et al., 2018a; Iudin et al., 2022). This intermittency is intrinsically linked to the fractal structure and critical dynamics of the lightning process (Bulatov et al., 2020; Gou et al., 2018b; Sterpka et al., 2021; Iudin & Syssoev, 2022; Syssoev et al., 2022). Additionally, the inherent polarity asymmetry in bidirectional leader development introduces instability in the discharge process, leading to destabilization and re-excitation phenomena in various lightning events (Van der Velde & Montanya, 2013; Williams, 2006; Williams & Heckman, 2012; Iudin, 2021; da Silva et al., 2023; Scholten et al., 2023).

32 The intermittent nature of lightning is particularly evident in ground flashes, where
33 negative ground flash discharges are characteristically separated by extended periods of dim
34 luminosity. These periods are marked by a distinctive sequence: when the downward negative
35 channel decays and eventually terminates, the still-active intracloud positive component
36 intermittently creates conditions that facilitate the formation of dart or dart-stepped leaders (Van
37 der Velde & Montanya, 2013; Stock et al., 2014; Stock et al., 2023; Lapierre et al., 2017; Jensen
38 et al., 2023). A similar intermittent behavior is observed in cloud flashes, where the active
39 positive leader exhibits marked temporal asymmetry compared to the negative leader, resulting
40 in K-processes or recoil leaders within the cloud. These transient phenomena are generally
41 attributed to channel instability, which manifests primarily through negative differential
42 resistance characteristics of the channel (Williams & Heckman, 2012; Mazur, 2016b).

43 In gas discharge physics, negative differential resistance is fundamentally associated with
44 bistability, hysteresis, and critical transitions (Bosch & Merlino, 1986; Lozneau et al., 2002;
45 Agop et al., 2012; Raizer & Mokrov, 2013). In lightning discharges, the leader and streamer
46 form a strongly coupled system with complex interactions: streamers supply the energy and
47 current essential for leader development, while the highly conductive leader channel maintains
48 the electric field and potential required for continuous streamer propagation. Given this intricate
49 coupling, this study expands the investigation of negative differential resistance properties to
50 encompass the entire leader-streamer system, rather than focusing solely on the leader channel.
51 Our analysis specifically examines the stability characteristics during lightning development and
52 identifies the critical conditions—in terms of current and potential difference—that govern
53 channel stability.

54 **2 Method**

55 **2.1 Negative differential resistance in lightning**

56 Lightning, as a natural large-scale arc discharge, exhibits negative differential resistance
57 characteristics in its channel (Heckman, 1992; da Silva et al., 2019). This behavior manifests
58 when channel temperature and conductivity increase with current, leading to a decrease in the
59 internal electric field needed to maintain the current, thus reducing the voltage across the channel
60 ($dV/dI < 0$). This characteristic was identified by Krehbiel et al. (1979) as a potential mechanism
61 for channel attenuation.

62 Heckman (1992) and Williams & Heckman (2012) investigated how negative differential
63 resistance relates to the multiplicity of negative ground flashes. They proposed that while a
64 channel with negative differential resistance connected to an extended streamer source is
65 inherently unstable, parallel channel resistance and capacitance could provide stabilization.
66 Specifically, channel stability occurs when the electrical response time constant (RC) exceeds
67 the thermal attenuation constant τ , with a critical stability current of approximately 100 A
68 (Heckman, 1992; Williams, 2006; Williams & Heckman, 2012).

69 However, Mazur & Ruhnke (2014) and Mazur (2016a, b) challenged the appropriateness
70 of modeling the leader channel as a parallel RC circuit. They argued that channel stability
71 depends primarily on the minimum potential difference in the streamer zone at the channel tip,
72 rather than negative differential resistance characteristics (Bazelyan & Raizer, 2000; Mazur,
73 2016a). Given that leader development is guided by numerous streamers at the front, we suggest
74 that differential resistance analysis should consider both the leader channel and its associated
75 streamers.

76 2.2 Negative differential resistance and bistability

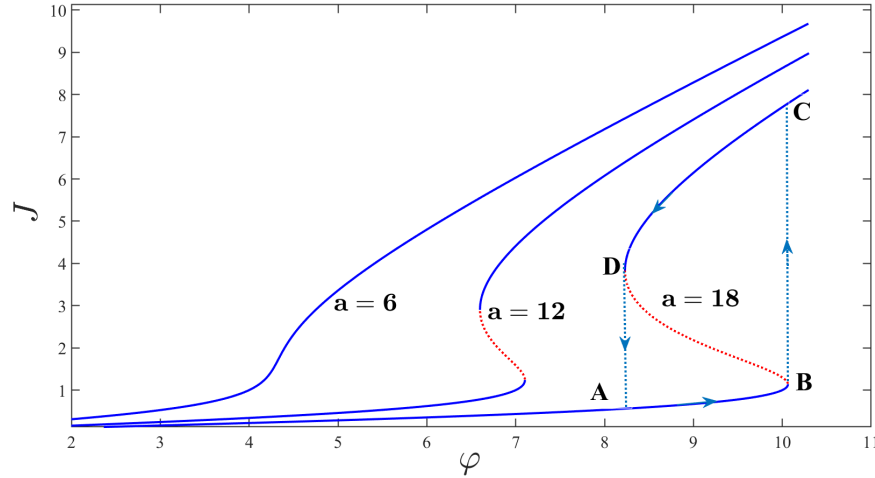
77 To understand how negative differential resistance leads to bistability in lightning
78 channels, we use a normalized relationship between current J and voltage φ that captures the
79 essential nonlinear dynamics of the discharge process. This relationship emerges from the
80 fundamental physics of plasma channel formation and maintenance (Agop et al., 2012):

$$81 \quad \varphi = J \left(1 + \frac{a}{1 + J^2} \right) \quad (1)$$

82 where a is a dimensionless control parameter that governs the system's nonlinear
83 characteristics

84 As illustrated in Figure 1, for parameter $a = 18$, the $J - \varphi$ characteristic curve exhibits
85 three distinct regions. There are two stable regions where $\varphi'(J) > 0$: a low-conductivity state
86 (segment AB) and a high-conductivity state (segment CD), both characterized by a
87 monotonically increasing current with voltage. These stable regions are separated by an unstable
88 region where $\varphi'(J) < 0$, demonstrating negative differential resistance. The system displays
89 bistability, with critical transitions occurring between the two stable states: at point B, the system

90 abruptly transitions from the low-conductivity state to the high-conductivity state, while at point
 91 D, it reverts to the low-conductivity state. This results in hysteretic behavior, where the system
 92 follows different paths during voltage increase (A→B→C) and decrease (C→D→A).



93
 94 Fig. 1. Theoretical dependence of the normalized current on the normalized potential (adapted from Agop et
 95 al., 2012, reprinted with permission from the Physical Society of Japan)

96 In nonlinear dynamics, negative differential resistance, bistability, and hysteresis are
 97 commonly observed. Considering the dynamic system $\frac{dJ}{dt} = f(\varphi, a, J)$, where J is the state
 98 variable and φ, a is a parameter. The equilibrium points are given by $f(\varphi, a, J) = 0$. At an
 99 equilibrium point, the system is unstable when $\partial f / \partial J > 0$ and stable when $\partial f / \partial J < 0$.

100 Let's define:

$$101 \quad f(\varphi, a, J) = \varphi - J \left(1 + \frac{a}{1 + J^2} \right) \quad (2)$$

102 Then

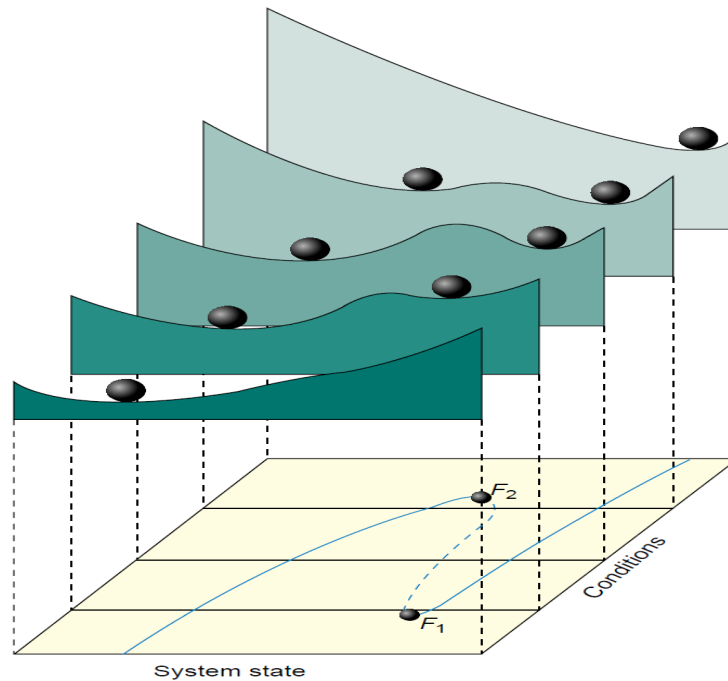
$$103 \quad \partial f / \partial J = -1 - a \frac{1 - J^2}{(1 + J^2)^2} \quad (3)$$

104 From equation (1), at equilibrium we have $\varphi = J \left(1 + \frac{a}{1 + J^2} \right)$, and $\partial f / \partial J = -\varphi' (J)$.

105 The stability condition $\partial f / \partial J > 0$ is equivalent to $\varphi' (J) < 0$, which corresponds to negative
 106 differential resistance. This mathematical analysis provides insight into how the sign of channel
 107 differential resistance determines the stability of lightning channel states and their transitions

108 Similar bistability, hysteresis, and critical transitions are widely observed in biological,
 109 atmospheric, ecological, and other systems, and they can be described by similar dynamical
 110 systems (Scheffer & Carpenter, 2003; Scheffer, 2009). The generation of instability and
 111 bistability can be illustrated by the rolling ball model shown in Figure 2, where the peaks and
 112 valleys represent unstable and stable points, respectively. Instability triggered by strong
 113 nonlinearities (positive feedback) is an important factor causing the bistability (polymorphism)
 114 of the system and the critical transition.

115



116

117 Fig. 2. Schematic representation of the locus of stability as a function of external conditions (adapted from
 118 Scheffer & Carpenter, 2003, reprinted with permission from Springer Nature)

119 **2.3 The relationship between Lightning channel electric field and current.**

120 The differential resistance characteristics of a gas discharge gap at a centimeter scale were
 121 measured first by King (1961). However, due to the effect of electrode vaporization, as pointed
 122 out by Mazur & Ruhnke (2014), King's results are only applicable to currents less than 10A with
 123 short gaps. In larger-scale lightning channels, the relationship between current and electric field
 124 is generally expressed in a power-law form. For example, Bazelyan et al. (2008) assumed that
 125 the leader channel current is inversely proportional to the electric field, $E = 3400I^{-1}$,

126 meanwhile, Larsson et al. (2005) proposed that the relationship between channel current and
127 electric field can be described as:

$$128 \quad E = 1600I^{-0.18} \quad (4)$$

129 This is consistent with the observations of Tanaka et al. (2003) and aligns with the
130 suggestions of da Silva et al. (2019) , who suggested that the power law varies for different
131 segments within the range of 10^2 to 10^4 A.

132 To develop a comprehensive description of the channel's electrical characteristics across
133 different current regimes, we combined two complementary datasets:

134 1. King et al. (1961) data for $I < 10$ A, characterizing the initial breakdown phase where
135 electrode effects dominate.

136 2. Larsson et al. (2005) measurements for $I > 10$ A, representing the fully developed
137 leader channel. The combined dataset was then fitted using a double power-law model that
138 captures both regimes

$$139 \quad E = aI^b + cI^d \quad (5)$$

140 Where $a = 4278$, $b = -0.9788$, $c = 1799$, $d = -0.2006$, The minimum current used for
141 fitting was approximately 0.1 A.

142 Figure 3 shows the relationship between the electric field and current, with squares
143 represent King's observations, circles representing Tanaka's (2003) experiments, and the solid
144 green line representing the fitted curve.

145

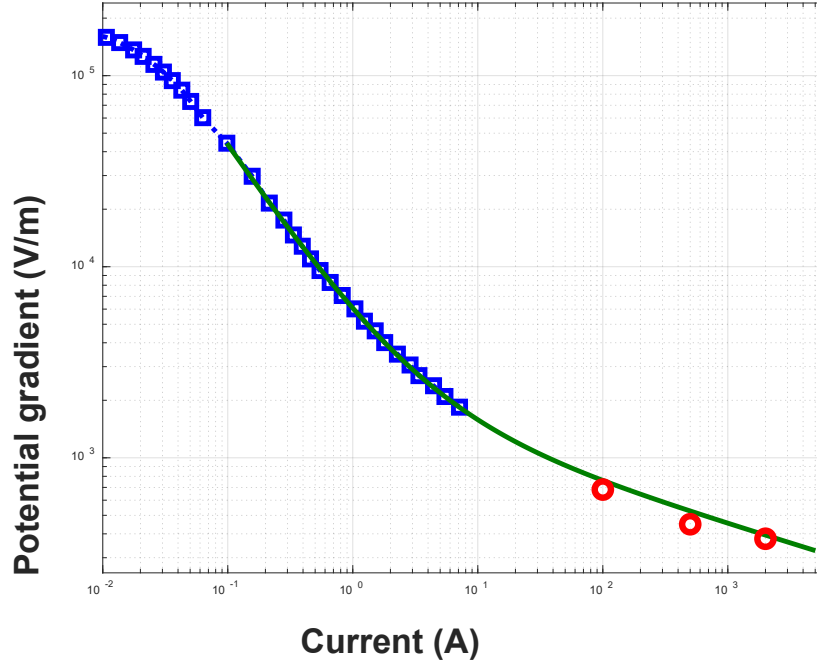


Fig. 3. Electric field versus current in arc channel

146
147
148
149

150 2.4 Differential resistance of the leader-streamer channel

151 The resistance of a streamer channel is determined by the potential difference ΔU_T across
152 the streamer zone of the leader head and the channel current I , which can be expressed as
153 (Bazelyan & Raizer, 2000):

$$154 \quad I = q_c V_L = 2\pi\epsilon_0 V_L \Delta U_T \quad (6)$$

155 where q_c represents the channel charge line density, and V_L is the channel development speed.
156 The relationship between V_L and I follows a power-law form (Bazelyan & Raizer, 2000; Popov,
157 2009):

$$158 \quad V_L = kI^\alpha \quad (7)$$

159 Since the power exponent α varies significantly in different studies, such as $\alpha \approx 1/3$
160 (Hutzler & Hutzler, 1982; Bazelyan et al., 2007) and $\alpha \approx 0.66$ (Kekez & Savic, 1983), this
161 study adopts $k = 1.88 \times 10^4$, $\alpha = 0.67$ based on more recent works (Andreev et al., 2008;
162 Popov, 2009; Bazelyan et al., 2009).

163 From Equations (6) and (7), we derive the voltage drop across the streamer zone at the
 164 leader head:

$$165 \quad \Delta U_T = \frac{I}{2\pi\epsilon_0 k I^\alpha} = \frac{I^{1-\alpha}}{2\pi\epsilon_0 k} \quad (8)$$

166 Considering the leader channel potential drop $U_C = LE$, where L is the leader channel
 167 length and E is the electric field of the channel as shown in Equation (4), and the streamer
 168 channel potential drop ΔU_T from Equation (8), the total potential drop U of the leader-
 169 streamer system is:

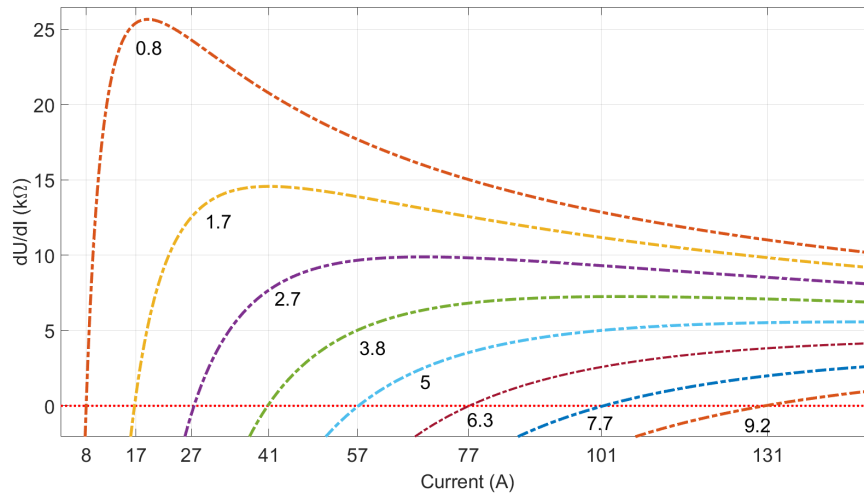
$$171 \quad U = L(aI^b + cI^d) + \frac{I^{1-\alpha}}{2\pi\epsilon_0 k} \quad (9)$$

172 Differentiating both sides with respect to I , we obtain the total differential resistance:

$$173 \quad \frac{dU}{dI} = L(abI^{b-1} + c d I^{d-1}) + (1 - \alpha) \frac{I^{-\alpha}}{2\pi\epsilon_0 k} \quad (10)$$

174 3 Analysis results

175 Figure 4 illustrates how the differential resistance varies with channel current for different
 176 leader channel lengths, where the horizontal line represents zero differential resistance. The point
 177 at which the curve intersects the horizontal line marks a change in the sign of the differential
 178 resistance, with the corresponding current at this intersection representing the critical current.



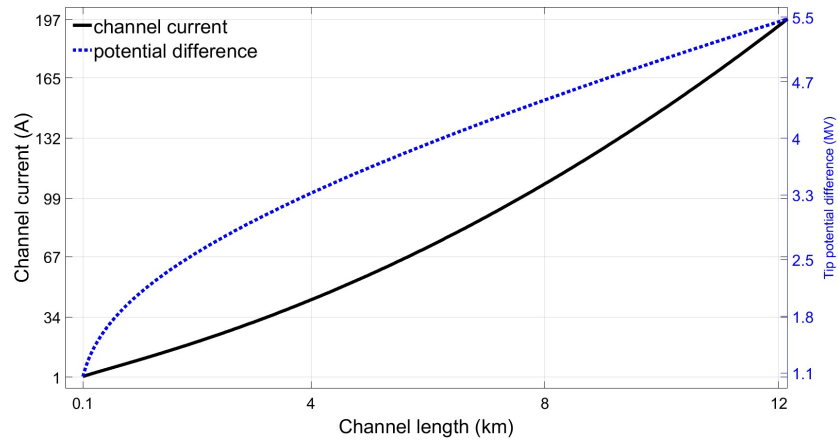
179

180 Fig. 4. Dependence of total differential resistance of channel on current with varying channel lengths (km).

181 The horizontal line represents zero resistance

182 Figure 5 shows that both the critical currents and the critical potential differences in the
183 streamer zone at the leader head increase with the channel length, which is consistent with
184 theoretical predictions. This trend aligns with Heckman's 1992 study on critical currents, and
185 supports the threshold condition for the critical potential difference proposed by Bazelyan &
186 Raizer (2000) and Mazur (2016a).

187



188

189 Fig. 5. Critical channel current and potential difference

190 of the streamer channel at the leader tip vary with channel length.

191 As the leader channel length increases, the ambient (stabilized) electric field decreases.

192 Between 0.1 km and 12 km, the stabilized leader-streamer field drops from 15.5 kV/m to 1.1

193 kV/m. This trend is consistent with the findings of Lalande et al. (2002) and Becerra & Vernon

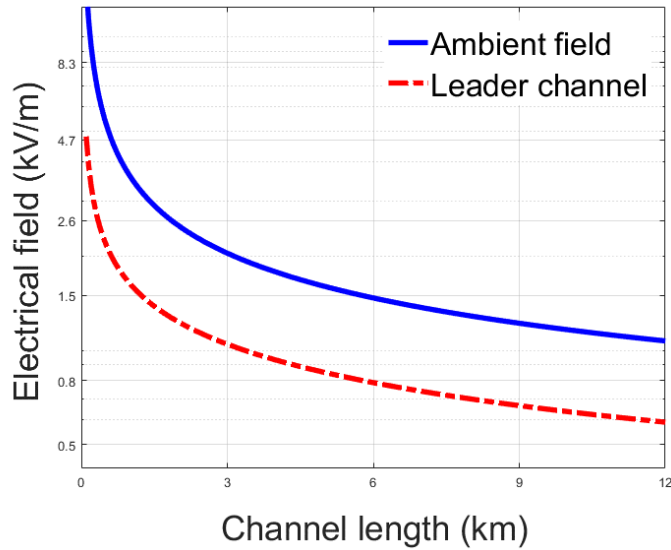
194 (2006) who reported that the leader channel's ambient electric field decreases with channel

195 height. Similarly, the internal electric field of the leader channel decreases (Figure 6). At a length

196 of 0.1 km, the electric field is approximately 4.9 kV/m, while at 12 km, it drops to 0.65 kV/m.

197 Syssoev & Shcherbakov (2001) found that stable thermal leader channels with long electric

198 fields (30–50 m) had electric fields around 3–10 kV/m, which is consistent with our results.



199 Fig. 6. variations of ambient electric field of the leader-streamer system and electric field of the leader
 200 channels with length
 201

202 **4 Discussion and conclusion**

203 This paper extends the discussion on lightning discharge channel stability and differential
 204 resistance from the leader channel to the leader-streamer system. Using bifurcation theory and
 205 critical transition theory from nonlinear dynamics, we studied the extinction, re-excitation, and
 206 critical transition of intermittent events (such as recoil leaders) in the lightning process. By
 207 analyzing the sign changes in the differential resistance of the leader-streamer system, we
 208 determined the critical current and the critical potential difference at the channel end. Our results
 209 show that as the channel length increases, both the critical current and the critical potential
 210 difference at the channel end increase. Meanwhile, the average ambient electric field and the
 211 electric field required for stable transmission gradually decrease after an initial sharp drop. These
 212 findings are consistent with existing research.

213 The exact mechanism behind the sudden change in channel conductivity remains unclear,
 214 but it is likely related to instability caused by positive feedback within the channel. The re-
 215 excitation of a decayed leader channel is typically due to the uneven distribution of current and
 216 electric field, which becomes more pronounced with increasing channel length. This asymmetry
 217 is particularly evident in the channel structure: the leader head maintains higher charge
 218 concentration and conductivity, remaining active and often merging with adjacent channels,

219 while the rear part exhibits lower conductivity and greater susceptibility to disconnection and
220 splitting

221 In the case of negative ground flashes, the electric field in the upper channel becomes
222 non-uniform due to the low current in the positive leader section, which is insufficient to
223 maintain conductivity in the lower channel. Recent observations show that the low current in the
224 positive leader and poor conductivity in the rear section lead to negative charge deposition in the
225 center of the rear channel. This creates negatively polarized needle structures that trigger
226 nonlinear instability (Williams & Montanya, 2019; Hare et al., 2019; Pu & Cummer, 2019; Hare
227 et al., 2021). The current in the rear positive leader decreases, leading to disconnection from the
228 negative leader. The increased potential difference at the paused negative leader causes re-
229 breakdown and reconnection, resulting in multiple strokes. In contrast, positive ground flashes
230 feature stronger current at the negative leader head, making the channel less prone to splitting,
231 which typically results in a single stroke.

232 The transition from a semiconductor to a conductive state in the leader channel may be
233 driven by ionization-thermal instability caused by positive feedback. As shown in previous
234 studies (Bazelyan & Raizer, 2000; Popov, 2009; da Silva et al., 2019), the pulsed mechanism of
235 the stepped leader is related to electric field inhomogeneity among the streamers at the leader
236 head (Syssoev & Iudin, 2023). This instability may exacerbate the electrical inhomogeneity in
237 the streamer zone, which is thought to be triggered by attachment instability (Douglas-Hamilton
238 & Mani, 1974; Sigmond, 1984; Luque et al., 2016; Malagón-Romero & Luque, 2019). If the
239 mechanism in positive stepped leaders is similar to that of negative stepped leaders, the
240 excitation of the leader should occur in the streamer zone at the leader head (Tran & Rakov,
241 2016; Kostinskiy et al., 2018; Huang et al., 2020; Wang et al., 2020).

242 Furthermore, the inhomogeneities, instabilities, and critical transitions observed in the
243 leader channel and streamer zone, whether during initiation or transmission, as well as the
244 emergence of pulse events of various scales and the interactions between leader channels,
245 streamers, and other streamers, all exhibit collective, fractal, and critical properties. These
246 phenomena may require more unified explanations based on fractal analysis and critical
247 dynamics.

248 **Acknowledgments**

249 The work leading to this paper was supported in part by the National Natural Science
250 Foundation of China (Grant No. 42065005, 42175100 and 42175090) and in part by The Hong
251 Kong Polytechnic University through the Research Grants Council of Hong Kong under Grant
252 GRF15215120

253 **Copyright and Permissions:**We affirm that all third-party copyrighted
254 material used in this manuscript has been obtained with proper permissions.
255 All such material is appropriately cited in the text and captions. Any
256 distribution licenses different from the standard CC BY (Creative Commons
257 Attribution) license are clearly stated below.

258 Figure 1: Adapted from "Experimental and Theoretical Investigations of the
259 Negative Differential Resistance in a Discharge Plasma," by Maricel Agop et
260 al., published in the Journal of the Physical Society of Japan. Used with
261 permission from the Physical Society of Japan. License: Non-commercial use
262 only.

263 Figure 2: Adapted from "Catastrophic regime shifts in ecosystems: linking
264 theory to observation," by Marten Scheffer and Stephen R. Carpenter, published
265 in Trends in Ecology & Evolution. Used with permission from Elsevier. License:
266 CC BY-NC.

267 Code/Data Availability

268 The data and code used in this study are available from the corresponding
269 author on reasonable request.

270 Author Contribution

- 271 • **Xueqiang Gou:** Conceptualization, Methodology, Software, Validation,
272 Formal analysis, Investigation, Writing – Original Draft, Review &
273 Editing, Visualization, Supervision, Project administration.
- 274 • **Chao Xin:** Software, Formal analysis,
- 275 • **Liwen Xu:** Visualization.
- 276 • **Ping Yuan, Yijun Zhang, Mingli Chen:** Review & Editing Supervision

277 Competing Interests

278 The authors declare that they have no known competing financial interests or
279 personal relationships that could have appeared to influence the work reported
280 in this paper.

281 **References**

282 Agop, M., Nica, P., Niculescu, O., and Dimitriu, D.-G.: Experimental and Theoretical
283 Investigations of the Negative Differential Resistance in a Discharge, *Plasma, Journal of the*
284 *Physical Society of Japan*, 81, 064502, <https://doi.org/10.1143/JPSJ.81.064502>, 2012.

285 Andreev, A. G., Bazelyan, E. M., Bulatov, M. U., Kuzhekin, I. P., Makalsky, L. M.,
286 Sukharevskij, D. I., and Syssoev, V. S.: Experimental study of the positive leader velocity as a
287 function of the current in the initial and final-jump phases of a spark discharge, *Plasma Physics*
288 *Reports*, 34, 609–615, <https://doi.org/10.1134/S1063780X0807009X>, 2008.

289 Bazelyan, E. M., Aleksandrov, N. L., Raizer, Yu P., and Konchakov, A. M.: The effect of
290 air density on atmospheric electric fields required for lightning initiation from a long airborne
291 object, *Atmospheric Research*, 86, 126–138, <https://doi.org/10.1016/j.atmosres.2007.03.007>,
292 2007.

293 Bazelyan, E. M., Raizer, Y. P., and Aleksandrov, N. L.: Corona initiated from grounded
294 objects under thunderstorm conditions and its influence on lightning attachment, *Plasma Sources*
295 *Science and Technology*, 17, 024015, <https://doi.org/10.1088/0963-0252/17/2/024015>, 2008.

296 Bazelyan, E., Syssoev, V., and Andreev, M.: Numerical simulations of spark channels
297 propagating along the ground surface: Comparison with high-current experiment, *Plasma*
298 *Physics Reports*, 35, <https://doi.org/10.1134/S1063780X0908011X>, 2009.

299 Becerra, M., and Cooray, V.: A simplified physical model to determine the lightning
300 upward connecting leader inception, *IEEE Trans. Power Delivery*, 21, 897–908,
301 <https://doi.org/10.1109/TPWRD.2005.858774>, 2006.

302 Bosch, R. A., and Merlino, R. L.: Sudden Jumps, Hysteresis, and Negative Resistance in
303 an Argon Plasma Discharge. I. Discharges with No Magnetic Field, *Beiträge aus der*
304 *Plasmaphysik*, 26, 1–12, <https://doi.org/10.1002/ctpp.19860260102>, 1986.

305 Bulatov, A. A., Iudin, D. I., and Syssoev, A. A.: Self-Organizing Transport Model of a
306 Spark Discharge in a Thunderstorm Cloud, *Radiophys Quantum El*, 63, 124–141,
307 <https://doi.org/10.1007/s11141-020-10041-z>, 2020.

308 da Silva, C. L., Sonnenfeld, R. G., Edens, H. E., Krehbiel, P. R., Quick, M. G., and
309 Koshak, W. J.: The plasma nature of lightning channels and the resulting nonlinear resistance,
310 *Journal of Geophysical Research: Atmospheres*, 124, 9442–9463,
311 <https://doi.org/10.1029/2019JD030693>, 2019.

312 da Silva, C. L., Winn, W. P., Taylor, M. C., Aulich, G. D., Hunyady, S. J., Eack, K. B., et
313 al.: Polarity asymmetries in rocket-triggered lightning, *Geophysical Research Letters*, 50,
314 e2023GL105041, <https://doi.org/10.1029/2023GL105041>, 2023.

315 Douglas-Hamilton, D. H., and Mani, S. A.: Attachment instability in an externally ionized
316 discharge, *J. Appl. Phys.*, 45, 4406, <https://doi.org/10.1063/1.1663065>, 1974.

317 Gou, X., Chen, M., Du, Y., and Dong, W.: Fractal dynamics analysis of the VHF radiation
318 pulses during initial breakdown process of lightning, *Geophysical Research Letters*, 37, L11808,
319 <https://doi.org/10.1029/2010GL043178>, 2010.

320 Gou, X., Chen, M., and Zhang, G.: Time correlations of lightning flash sequences in
321 thunderstorms revealed by fractal analysis, *Journal of Geophysical Research: Atmospheres*, 123,
322 <https://doi.org/10.1002/2017JD027206>, 2018.

323 Gou, X., Zhang, Y., Li, Y., et al.: Theory and observation of bidirectional leader of
324 lightning: Polarity asymmetry, instability, and intermittency, *Acta Physica Sinica*, 67, 205201,
325 <https://doi.org/10.7498/aps.67.20181079>, 2018.

326 Hare, B. M., Scholten, O., Dwyer, J., Strepka, C., Buitink, S., Corstanje, A., et al.: Needle
327 propagation and twinkling characteristics, *Journal of Geophysical Research: Atmospheres*, 126,
328 e2020JD034252, <https://doi.org/10.1029/2020JD034252>, 2021.

329 Heckman, S.: Why does a lightning flash have multiple strokes? PhD Thesis, Department
330 of Earth, Atmospheric and Planetary Sciences, Massachusetts Institute of Technology, 1992.

331 Huang, S., Chen, W., Pei, Z., Fu, Z., Wang, L., He, T., et al.: The discharge preceding the
332 intense reillumination in positive leader steps under the slow varying ambient electric field,
333 *Geophysical Research Letters*, 47, e2019GL086183, <https://doi.org/10.1029/2019GL086183>,
334 2020.

335 Hutzler, B., and Hutzler, D.: EDF Bull. Dir. Etudes Reck. (serie B), 4, 11–39, 1982.

336 Iudin, D. I., Sysoev, A. A., and Rakov, V.: Problems of Lightning Initiation and
337 Development, *Radiophys Quantum El*, 64, 780–803, <https://doi.org/10.1007/s11141-022-10178->
338 z, 2022.

339 Iudin, D. I., and Syssoev, A. A.: Hot Plasma Channel Network Formation in
340 Thunderclouds, *Journal of Atmospheric and Solar-Terrestrial Physics*, 240, 105944,
341 <https://doi.org/10.1016/j.jastp.2022.105944>, 2022.

342 Iudin, D.: Lightning as an Asymmetric Branching Network, *Atmospheric Research*,
343 <https://doi.org/10.1016/j.atmosres.2021.105560>, 2021.

344 Jensen, D., Shao, X. M., and Sonnenfeld, R.: Insights into Lightning K-Leader Initiation
345 and Development from Three Dimensional Broadband Interferometric Observations, *ESS Open*
346 *Archive*, <https://doi.org/10.22541/essoar.168275995.55801872/v2>, 2023.

347 Kekez, M., and Savic, P.: Correlation leader velocity for current varying from 90 mA to 2
348 kA, Report 4-th Inter. Symp. On High Voltage Engineering, Athens, 5–9 Sept., N 45.04, 1983.

349 King, L. A.: The voltage gradient of the free burning arc in air and nitrogen, in *Proc. Fifth*
350 *Intl. Conference on Ionization Phenomena in Gases*, 2, 871–877, North-Holland, Munich, 1961.

351 Kostinskiy, A. Y., Syssoev, V. S., Bogatov, N. A., Mareev, E. A., Andreev, M. G.,
352 Bulatov, M. U., et al.: Abrupt elongation (stepping) of negative and positive leaders culminating
353 in an intense corona streamer burst: Observations in long sparks and implications for lightning,
354 *Journal of Geophysical Research: Atmospheres*, 123, 5360–5375,
355 <https://doi.org/10.1029/2017JD027997>, 2018.

356 Krehbiel, P. R., Brook, M., and McCrory, R. A.: An analysis of the charge structure of
357 lightning discharges to ground, *Journal of Geophysical Research*, 84, 2432–2456,
358 <https://doi.org/10.1029/JC084iC05p02432>, 1979.

359 Lapierre, J. L., Sonnenfeld, R. G., Stock, M., Krehbiel, P. R., Edens, H. E., and Jensen,
360 D.: Expanding on the relationship between continuing current and in-cloud leader growth,
361 *Journal of Geophysical Research: Atmospheres*, 122, 4150–4164,
362 <https://doi.org/10.1002/2016JD026189>, 2017.

363 Lalande, P., Bondiou-Clergerie, A., Bacchiega, G., and Gallimberti, I.: Observations and
364 modeling of lightning leaders, *Comptes Rendus Physique*, 3, 1375–1392,
365 [https://doi.org/10.1016/S1631-0705\(02\)01413-5](https://doi.org/10.1016/S1631-0705(02)01413-5), 2002.

366 Larsson, A., Delannoy, A., and Lalande, P.: Voltage drop along a lightning channel during
367 strikes to aircraft, *Atmospheric Research*, 76, 377–385,
368 <https://doi.org/10.1016/j.atmosres.2004.11.032>, 2005.

369 Lozneau, E., Popescu, V., and Sanduloviciu, M.: Negative differential resistance related
370 to self-organization phenomena in a dc gas discharge, *Journal of Applied Physics*, 92, 1195–
371 1199, <https://doi.org/10.1063/1.1487456>, 2002.

372 Luque, A., Stenbaek-Nielsen, H. C., McHarg, M. G., and Haaland, R. K.: Sprite beads and
373 glows arising from the attachment instability in streamer channels, *Journal of Geophysical*
374 *Research: Space Physics*, 121, <https://doi.org/10.1002/2015JA022234>, 2016.

375 Malagón-Romero, A., and Luque, A.: Spontaneous emergence of space stems ahead of
376 negative leaders in lightning and long sparks, *Geophysical Research Letters*, 46, 4029–4038,
377 <https://doi.org/10.1029/2019GL082063>, 2019.

378 Malagón Romero, A. F.: Numerical investigation on the advance of leader channels in
379 lightning and long sparks, Universidad de Granada, 2021.

380 Mazur, V., and Ruhnke, L. H.: The physical processes of current cutoff in lightning
381 leaders, *Journal of Geophysical Research: Atmospheres*, 119, 2796–2810,
382 <https://doi.org/10.1002/2013JD020494>, 2014.

383 Mazur, V.: *Principles of Lightning Physics* (Bristol: IOP Publishing), pp1–183, 2016.

384 Mazur, V.: The physical concept of recoil leader formation, *Journal of Electrostatics*, 82,
385 79–87, <https://doi.org/10.1016/j.elstat.2016.05.003>, 2016.

386 Popov, N. A.: Study of the formation and propagation of a leader channel in air, *Plasma*
387 *Physics Reports*, 35, 785, <https://doi.org/10.1134/S1063780X0909005X>, 2009.

388 Pu, Y., and Cummer, S. A.: Needles and lightning leader dynamics imaged with 100–200
389 MHz broadband VHF interferometry, *Geophysical Research Letters*, 46, 13556–13563,
390 <https://doi.org/10.1029/2019GL085635>, 2019.

391 Raizer, Y. P., and Mokrov, M. S.: Physical mechanisms of self-organization and
392 formation of current patterns in gas discharges of the Townsend and glow types, *Physics of*
393 *Plasmas*, 20, 101604, <https://doi.org/10.1063/1.4825234>, 2013.

394 Scheffer, M., and Carpenter, S. R.: Catastrophic regime shifts in ecosystems: linking
395 theory to observation, *Trends in Ecology & Evolution*, 18, 648–656,
396 <https://doi.org/10.1016/j.tree.2003.09.002>, 2003.

397 Scheffer, M.: *Critical Transitions in Nature and Society* (Vol. 16), Princeton University
398 Press, 2009.

399 Scholten, O., Hare, B., Dwyer, J., et al.: Searching for intra-cloud positive leaders in VHF,
400 Research Square, <https://doi.org/10.21203/rs.3.rs-2631381/v1>, 2023.

401 Sterpka, C., Dwyer, J., Liu, N., Hare, B. M., Scholten, O., Buitink, S., and Nelles, A.: The
402 Spontaneous Nature of Lightning Initiation Revealed, *Geophysical Research Letters*, 48,
403 e2021GL095511, <https://doi.org/10.1029/2021GL095511>, 2021.

404 Sigmond, R. S.: The residual streamer channel: Return strokes and secondary streamers, *J.*
405 *Appl. Phys.*, 56, 1355–1370, <https://doi.org/10.1063/1.334126>, 1984.

406 Stock, M. G., Akita, M., Krehbiel, P. R., Rison, W., Edens, H. E., Kawasaki, Z., and
407 Stanley, M. A.: Continuous broadband digital interferometry of lightning using a generalized
408 across-correlation algorithm, *Journal of Geophysical Research: Atmospheres*, 119, 3134–3165,
409 <https://doi.org/10.1002/2013JD020217>, 2014.

410 Stock, M., Tilles, J., Taylor, G. B., Dowell, J., and Liu, N.: Lightning Interferometry with
411 the Long Wavelength Array, *Remote Sensing*, 15, 3657, <https://doi.org/10.3390/rs15143657>,
412 2023.

413 Syssoev, V. S., and Shcherbakov, Yu. V.: Electrical strength of ultra-long air gaps, in
414 *Proc. 2001 Int. Conf. on Lightning and Static Electricity*, Seattle, Washington, ID: SAE-2001-
415 01-2898, 2001.

416 Syssoev, A. A., Iudin, D. I., Iudin, F. D., Klimashov, V. Y., and Emelyanov, A. A.: Relay
417 charge transport in thunderclouds and its role in lightning initiation, *Scientific Reports*, 12, 1–21,
418 <https://doi.org/10.1038/s41598-022-10722-x>, 2022.

419 Syssoev, A. A., and Iudin, D. I.: Numerical Simulation of Electric Field Distribution
420 inside Streamer Zones of Positive and Negative Lightning Leaders, *Atmospheric Research*, 295,
421 107021, <https://doi.org/10.1016/j.atmosres.2023.107021>, 2023.

422 Tanaka, S.-I., Sunabe, K.-Y., and Goda, Y.: Internal voltage gradient and behavior of
423 column on long-gap DC free arc, *Electrical Engineering in Japan*, 144, 8–16,
424 <https://doi.org/10.1002/eej.10300>, 2003.

425 Tran, M. D., and Rakov, V. A.: Initiation and propagation of cloud-to-ground lightning
426 observed with a high-speed video camera, *Scientific Reports*, 6, 39521,
427 <https://doi.org/10.1038/srep39521>, 2016.

428 Van der Velde, O. A., and Montanya, J.: Asymmetries in bidirectional leader development
429 of lightning flashes, *Journal of Geophysical Research: Atmospheres*, 118, 13504–13519,
430 <https://doi.org/10.1002/2013JD020257>, 2013.

431 Wang, X., Wang, D., He, J., and Takagi, N.: A comparative study on the discontinuous
432 luminosities of two upward lightning leaders with opposite polarities, *Journal of Geophysical*
433 *Research: Atmospheres*, 125, e2020JD032533, <https://doi.org/10.1029/2020JD032533>, 2020.

434 Williams, E. R.: Problems in lightning physics - the role of polarity asymmetry, *Plasma*
435 *Sources Sci. Technol.*, 15, S91, <https://doi.org/10.1088/0963-0252/15/2/S01>, 2006.

436 Williams, E., and Heckman, S.: Polarity asymmetry in lightning leaders: The evolution of
437 ideas on lightning behavior from strikes to aircraft, *Aerospace Lab Journal*, 5, A105-04, 1–8,
438 2012.

439 Williams, E., and Montanya, J.: A closer look at lightning reveals needle-like structures,
440 *Nature*, 568, 319–320, <https://doi.org/10.1038/d41586-019-01178-7>, 2019.